THE JOURNAL OF PHYSICAL CHEMISTRY C LETTERS

2008, *112,* 18287–18290
Published on Web 10/23/2008

Surface Structure of KIO_3 Grown by Heterogeneous Reaction of Ozone with KI (001)

Matthew A. Brown,[†] Zhi Liu,[‡] Paul D. Ashby,[§] Apurva Mehta,[||] Ronald L. Grimm,[†] and John C. Hemminger*,[†]

Department of Chemistry, University of California, Irvine, California 92697, Advanced Light Source, Lawrence Berkeley National Laboratory, Berkeley, California 94720, Molecular Foundry, Lawrence Berkeley National Laboratory, Berkeley, California 94720, and Stanford Synchrotron Radiation Laboratory, Stanford Linear Accelerator Center, Menlo Park, California 94025

Received: August 8, 2008

The crystal structure of KIO_3 grown by heterogeneous surface oxidation of KI (001) with ozone is reported. Under ambient reaction conditions (RH ~35%, room temperature) a thick layer of KIO_3 grows at the gas−solid interface. Two doublets are present in the I(4d) X-ray photoelectron spectroscopy structure measurements, characteristic of unreacted KI (I^-) from the substrate and the oxidized KIO_3 (I^{5+}) reaction product. X-ray diffraction measurements confirm the presence at the interface of randomly oriented polycrystalline-triclinic KIO_3 with an average particle diameter of 15 nm. KIO_3 particle diameters determined from the X-ray diffraction peak widths are consistent with the results of atomic force microscopy. There is no X-ray powder diffraction evidence to suggest that the underlying KI substrate is altered in any manner during this heterogeneous interfacial reaction.

Introduction

Heterogeneous interfacial chemistry has become an important element of atmospheric science, with particular attention given to halogens and halogenated oxides because they play prominent roles in regulating the lifetimes of many reactive trace gases, including ozone.[1–3] Field studies have shown the concentration of certain halogenated compounds to exceed theoretical predictions based on simple source models,[4–6] with the inference that some gaseous inorganic halides are directly delivered to the free troposphere by sea-salt aerosol.[1,3] Although the mechanisms of halogen release from aerosol particles are presently not well-understood, heterogeneous oxidation of halide components in sea-salt aerosol have been proposed for their release in the marine boundary layer.

In light of the complexity of sea-salt aerosols (chemical composition, topography and structure), and the corresponding difficulty in determining reaction mechanisms of halide release, studies employing simple alkali halides as mimics of sea-salt aerosol have been reported in the literature. These model systems allow fundamental investigations that can often elucidate microscopic chemical composition, kinetic rate information, reaction mechanisms, and surface topography with the rigor of modern surface science, while representing the reactivity and chemical specificity of the individual constituents of sea-salt aerosol. Many of these studies have focused on alkali iodides in aqueous solution following theoretical predictions of increased iodide concentration at the free-surface in neat water.[7] Interfacial enhancement of I^- in neat aqueous electrolyte solutions of KI[8] and NaI,[9] and in ternary KI aqueous solution coated with an organic surfactant layer,[10] have been reported in the literature.

Heterogeneous surface reactivity measurements of alkali iodides with trace atmospheric oxidants under vacuum conditions remain more scarce in the literature,[11–14] but represent a critical resource for understanding complex interfacial chemical reactions on a microscopic scale. Our previous publications have focused on the surface oxidation of dry KI (001) by ozone. Electronic structure measurements using X-ray photoelectron spectroscopy (XPS) have shown the reaction to be self-passivating, creating a stable layer of KIO_3 with an average reactive sticking coefficient of 1.4 ($\pm$0.7) $\times$ 10^{-4}.[13] Atomic force microscopy (AFM) studies have shown the reaction to initiate at step edge and defect sites along the KI (001) plane prior to propagating across sample terraces.[12] Enami et al. have also demonstrated the catalytic activity of iodide in the oxidation and subsequent release of bromide and chloride in aqueous nanodroplets exposed to ozone.[14] These studies conclude that iodide-containing particles, both crystalline and aqueous nanodroplets are sinks for ozone and must be accounted for in kinetic models of atmospheric chemistry.

Herein, we present an X-ray diffraction (XRD) surface structure study of the reacting interface and report the crystal structure of the final KIO_3 layer grown by heterogeneous oxidation of KI (001) with ozone under ambient laboratory conditions. XRD, XPS and AFM results indicate the final reaction product consists of a surface layer of randomly oriented polycrystalline-triclinic KIO_3 with an average particle diameter of 15 nm residing at the interface of the unaltered KI substrate.

Experimental Section

Solid samples of KI (Hilger, U.K.) were prepared by cleavage along the 001 plane and transferred to a small reaction vessel.

* Corresponding author. E-mail: jchemmin@uci.edu.
[†] University of California, Irvine.
[‡] Advanced Light Source, Lawrence Berkeley National Laboratory.
[§] Molecular Foundry, Lawrence Berkeley National Laboratory.
[||] Stanford Linear Accelerator Center.

10.1021/jp807113d CCC: $40.75

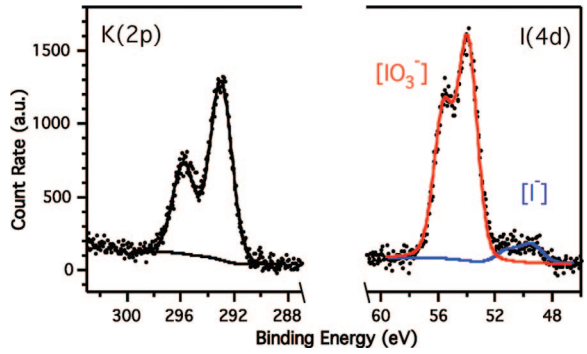

Figure 1. XPS results show the presence of two I(4d) doublets separated by 4.9 eV at characteristic binding energies of I^- (48.8 eV) and I^{5+} (53.7 eV) in KI and KIO_3, respectively. A single electronic K(2p) component is observed. The binding energy scale is relative to the K($2p_{3/2}$) set at 292.8 eV.[15]

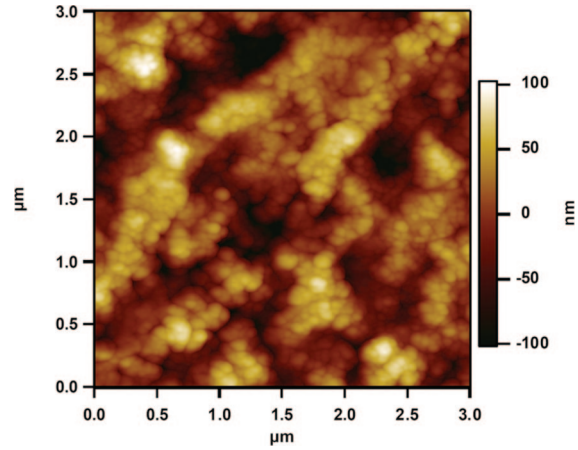

Figure 2. Topographic repulsive-mode tapping image of the KI (001) surface following oxidation by ozone under ambient laboratory conditions. The surface is covered in an inhomogeneous oxide layer of KIO_3 and is roughened significantly from that of the original KI (001) plane.

Ozone exposures were carried out under ambient (RH ~ 35%) conditions at 1 atm total pressure for 2 h. Ozone concentrations were 147 mg/L in oxygen. Following oxidation the samples were analyzed via XPS, AFM and XRD.

XPS peak areas for I(4d) and K(2p) were measured from spectra collected with a PHI 5400 surface analysis instrument using Al Kα incident radiation (1486.6 eV) following a standard Shirley background subtraction. Peak positions were referenced to the K($2p_{3/2}$) of the original KI (001) starting material (292.8 eV).[15]

Topographic images were collected on a commercial Asylum Research MFP3D instrument in the repulsive regime of AC mode using highly doped silicon tips (Budget Sensors) with a force constant of 3 N/m. AFM measurements were carried out in a modified version of a commercial liquid cell where the relative humidity was below 4% at a total cell pressure of 1 atm and 293 K.

XRD patterns were collected at beamline 11-3 of the Stanford Synchrotron Radiation Laboratory (SLAC) using monochromatic incident radiation of 12.7 keV. Diffraction patterns were collected at a grazing incidence angle of 0.5° using a large area detector. Under the geometry of this experiment the X-ray penetration length into the sample is 362 nm.[16] The 2d images were processed and transformed into diffraction space using the software, Area Diffraction Machine.[17] A custom-made sample holder with Kapton windows housed the sample and was purged in argon throughout the measurements to limit the humidity above the sample surface. The diffraction pattern from a freshly cleaved KI (001) sample was collected as reference. A diffraction pattern of powdered LaB_6 was collected in the same geometry and used for calibration of Q space.

Results and Discussion

The reaction of ozone with solid KI to form KIO_3 is thermodynamically favored according to the reaction

$$KI_{(s)} + 3O_{3(g)} \rightarrow KIO_{3(s)} + 3O_{2(g)}$$

with a room temperature $\Delta G^o_{rxn} = -579$ kJ/mol.[18] The continued reaction to form potassium periodate (KIO_4) is further energetically favored with a $\Delta G^o_{rxn} = -685$ kJ/mol.[18] Figure 1 shows the XP spectrum of the K(2p) and I(4d) regions following reaction under ambient conditions with ozone. The binding energy of the K($2p_{3/2}$) has been set at 292.8 eV for reference, characteristic of the original KI (001) starting material.[15] There is a single K(2p) electronic state in the spectrum, while the I(4d) region is composed of two doublets (spin orbit splitting (SOS) of the 4d orbital results in a doublet for each electronic state with an SOS = 1.69 eV).[19] The low binding energy peak at 48.8 eV is assigned to the unreacted I^-(4d) of the original KI (001) and the high binding energy peak, shifted by 4.9 eV is assigned to the I^{5+}(4d) of the oxidized KIO_3.[13,15] There is no XPS evidence for the formation of a periodate (KIO_4 (I^{7+} oxidation state)) reaction product. There is also no spectroscopic evidence of intermediate iodide oxidation states in the formation of the final KIO_3 product (i.e., KIO, KIO_2); however, we cannot rule them out as short-lived intermediates in the formation of the stable KIO_3 product.

Under the oxidation conditions of this experiment (RH ~35%) there is significantly more KIO_3 on the surface than we previously reported for KI (001) samples oxidized under controlled ultrahigh vacuum (UHV) conditions. [13] Here, an IO_3^-/I^- ratio of 10.85 is obtained, whereas we have previously reported saturation IO_3^-/I^- ratios of 0.30 for samples grown under UHV conditions.[13] Details of the KIO_3 oxide growth as a function of relative humidity will be covered in a separate publication;[20] here we focus on identifying the crystal structure of the KIO_3 reaction product layer.

The topography of the surface KIO_3 layer is shown in Figure 2. Consistent with the XPS results (Figure 1), a thick oxide layer is formed. Particle aggregates on the order of hundreds of nanometers in size are inhomogeneously distributed around the sample surface.[12] Individual particles in the aggregates typically measure a few tens of nanometers but may be as large as 80 nm in diameter. Accurate lateral dimensions are difficult to estimate as a result of the AFM tip-shape. The KIO_3 surface layer has an rms roughness of 36.6 nm, whereas we have previously reported an rms roughness of 0.3 Å, mostly the result of instrument noise, for a freshly cleaved KI (001) surface, and an rms roughness of 3.2 nm for a KIO_3 oxide layer grown under dry reaction conditions. The size and distribution of KIO_3 particles in this study vary greatly from the results of our study under dry oxidation conditions. KIO_3 particles grown under a controlled humidity below 4% had a narrow distribution, with widths typically of 10−30 nm and heights of only 4−6 nm.[12]

The collected XRD pattern is shown as an inset in Figure 3, whereas the rest of the figure shows the azimuthally integrated diffraction pattern in Q space (summarized in Table 1). For comparison the reference patterns of KI (ICDD, no. 01-089-3621)[21] and KIO_3 (ICDD, no. 01-77-1241)[22] are plotted in blue

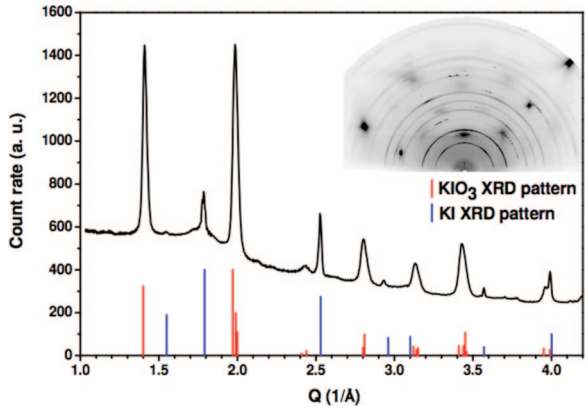

Figure 3. Integrated azimuthal diffraction pattern in Q space. The inset displays the collected XRD pattern, whereas the reference patterns of KI and KIO_3 are shown in the bottom. The collect pattern confirms the presence of polycrystalline KIO_3 with a random surface orientation.

TABLE 1: Summary of X-ray Diffraction Pattern in Q Space Where the Markers Indicate to Which Crystal Structure (KI or KIO_3) the Peaks Have Been Assigned

Q (1/Å)	KI[21]	KIO_3[22]
1.40		•
1.79	•	
1.99		•
2.42		•
2.53	•	
2.81		•
2.92	•	
3.15		•
3.42		•
3.58	•	
3.95		•
4.00	•	

and red, respectively, at the bottom of Figure 3. The only two crystalline structures present at the interface in the collected XRD pattern are those of KI and KIO_3. There are no diffraction lines for the more thermodynamically favored KIO_4 product. The KI (001) diffraction line of the substrate is present at $Q = 1.79$, residing on a broad diffuse background characteristic of substrate patterns. Other lower intensity substrate peaks are also present throughout the diffraction pattern as discontinuous sharp rings. These diffraction peaks were present in a freshly cleaved KI sample prior to reaction with ozone, used as a reference pattern. There is no change beyond an attenuation of the intensity (a result of a surface layer of KIO_3 covering the KI substrate), in the KI substrate diffraction pattern following reaction with ozone to form KIO_3. That is, the surface reaction forming a passivating layer of potassium iodate does not modify the surface structure of the KI substrate. The majority phase in the diffraction pattern is that of polycrystalline-triclinic KIO_3. The diffraction rings of KIO_3 are continuous and slightly textured, which indicates that the polycrystalline-triclinic KIO_3 particles are randomly orientated with little preferred growth orientation at the interface of the KI (001) substrate. An average KIO_3 particle diameter of 14.7 (±0.5) nm is calculated using the Sherrer equation, consistent with the results of the AFM imaging (shown in Figure 2). It is important to note that the results of the XRD analysis, which provide a diffraction fingerprint of the reacting interface, further confirm the XPS results of this and our previous study[13] in that there is no evidence for the formation of a KIO_4 reaction product under the conditions of this experiment.

Conclusion

A combined surface-specific study provides evidence of interfacial potassium iodate, KIO_3, formation under ambient conditions for the heterogeneous reaction $KI_{(s)} + 3O_{3(g)} \rightarrow KIO_{3(s)} + 3O_{2(g)}$. XPS results reveal two distinct I(4d) electronic states, assigned to the I^- of the original unreacted KI, and to the I^{5+} of the KIO_3 oxide layer. AFM micrographs confirm the results of the XPS measurements in terms of a thick oxide layer with particles as large as 80 nm in diameter. XRD patterns further confirm the reacting interface contains only the crystal structures of KI and KIO_3, with the majority phase that of randomly oriented polycrystalline-triclinic KIO_3. An average KIO_3 particle diameter of 14.7 (±0.5) nm is calculated from the diffraction pattern in agreement with the majority of particles measured by AFM. The X-ray diffraction pattern suggests that this interfacial heterogeneous reaction does not modify the crystal structure of the underlying KI substrate. Our study provides the first crystal structure measurement of KIO_3 formed by heterogeneous reaction of KI (001) with ozone and demonstrates that the resulting potassium iodate product is randomly oriented at the interface. We also confirm that there is no formation of the more thermodynamically stable KIO_4 product under the conditions of our experiments.

Acknowledgment. The AirUCI Environmental Molecular Sciences Institute under grant no. CHE 0431312 from the National Science Foundation supported this work. Portions of this work were performed at the Molecular Foundry, LBNL, which is supported by the Office of Science, Office of Basic Energy Sciences, of the U.S. Department of Energy under contract no. DE-AC0205CH11231. XRD patterns were collected at SSRL, SLAC, which is supported by the Office of Science, Office of Basic Energy Sciences, of the U.S. Department of Energy under contract no. DE-AC0376SF000515. M.A.B. is grateful to Ron Hulme for machining the XRD sample holder, and acknowledges the ALS Doctoral Fellowship program.

References and Notes

(1) Finlayson-Pitts, B. J., Jr. *Chemistry of the Upper and Lower Atmosphere*; Academic Press: New York, 2000.
(2) Seinfeld, J. H.; Pandis, S. N. Atmospheric chemistry and physics: from air pollution to climate change; Wiley: New York, 1998.
(3) Finlayson-Pitts, B. J.; Hemminger, J. C. *J. Phys. Chem. A* **2000**, *104*, 11463.
(4) Sioris, C. E.; Kovalenko, L. J.; McLinden, C. A.; Salawitch, R. J.; Van Roozendael, M.; Goutail, F.; Dorf, M.; Pfeilsticker, K.; Chance, K.; von Savigny, C.; Liu, X.; Kurosu, T. P.; Pommereau, J. P.; Bosch, H.; Frerick, J. *J. Geophys. Res.-Atmos.* **2006**, *111*.
(5) Dorf, M.; Butler, J. H.; Butz, A.; Camy-Peyret, C.; Chipperfield, M. P.; Kritten, L.; Montzka, S. A.; Simmes, B.; Weidner, F.; Pfeilsticker, K. *Geophys. Res. Lett.* **2006**, *33*.
(6) Saiz-Lopez, A.; Plane, J. M. C. *Geophys. Res. Lett.* **2004**, *31*.
(7) Jungwirth, P.; Tobias, D. J. *Chem. Rev.* **2006**, *106*, 1259.
(8) (a) Ghosal, S.; Hemminger, J. C.; Bluhm, H.; Mun, B. S.; Hebenstreit, E. L. D.; Ketteler, G.; Ogletree, D. F.; Requejo, F. G.; Salmeron, M. *Science* **2005**, *307*, 563. (b) Brown, M. A.; D′Auria, R.; Kuo, I. -F. W.; Krisch, M. J.; Starr, D. E.; Bluhm, H.; Tobias, D. J.; Hemminger, J. C. *Phys. Chem. Chem. Phys.* **2008**, *10*, 4778.
(9) Petersen, P. B.; Johnson, J. C.; Knutsen, K. P.; Saykally, R. J. *Chem. Phys. Lett.* **2004**, *397*, 46.
(10) Krisch, M. J.; D'Auria, R.; Brown, M. A.; Starr, D. E.; Bluhm, H.; Tobias, D. J.; Hemminger, J. C. *J. Phys. Chem. C* **2007**, *111*, 13497.
(11) Brown, M. A.; Johanek, V.; Hemminger, J. C. *Rev. Sci. Instrum.* **2008**, *79*, 02410.
(12) Brown, M. A.; Ashby, P. D.; Ogeltree, D. F.; Salmeron, M.; Hemminger, J. C. *J. Phys. Chem. C* **2008**, *112*, 8110.
(13) Brown, M. A.; Newberg, J. T.; Krisch, M. J.; Mun, B. S.; Hemminger, J. C. *J. Phys. Chem. C* **2008**, *112*, 5520.
(14) Enami, S.; Vecitis, C. D.; Cheng, J.; Hoffmann, M. R.; Colussi, A. J. *J. Phys. Chem. A* **2007**, *111*, 8749.

(15) Morgan, W. E.; Stec, W. J.; Vanwazer, J. R. *J. Am. Chem. Soc.* **1973**, *95*, 751.
(16) Centre for X-ray Optics, LBNL; http://www-cxro.lbl.gov.
(17) Lande, J.; Webb, S.; Bronfenbrenner, D.; and Mehta, A. Area Diffraction Machine; http://code.google.com/p/areadiffractionmachine/
(18) Lide, D. R. *Handbook of Chemistry and Physics*; CRC Press: Cleveland, OH, 2004.
(19) Bearden, J. A.; Burr, A. F. *Rev. Mod. Phys.* **1967**, *39*, 125.
(20) Brown, M. A. Interfacial Chemistry of Alkali Halides. Ph.D. Thesis, Department of Chemistry, University of California, Irvine, CA, 92697, 2008.
(21) Cortona, P. *Phys. Rev. B* **1992**, *46*, 2008.
(22) Lucas, B. W. *Acta Crystallogr., Sect. C-Cryst. Struct. Commun.* **1984**, *40*, 1989.

JP807113D